

1 **An Integrated Germline and Somatic Genomic Model Improves Risk Prediction for Coronary**  
2 **Artery Disease**  
3

4 Xiong Yang<sup>1,2,\*</sup>, Min Seo Kim<sup>3,4,\*</sup>, Xinyu Zhu<sup>1,2,5</sup>, Md Mesbah Uddin<sup>3,4</sup>, Tetsushi Nakao<sup>3,4,6,7</sup>, So  
5 Mi Jemma Cho<sup>3,4</sup>, Satoshi Koyama<sup>3,4</sup>, Tingfeng Xu<sup>1,2,5</sup>, Laurens F. Reeskamp<sup>3,8,9</sup>, Rufan Zhang<sup>1,2</sup>,  
6 Zhaoqi Liu<sup>1,2,5</sup>, Yunga A<sup>1,2,5</sup>, Paul S. de Vries<sup>10</sup>, Ramachandran S. Vasan<sup>11,12</sup>, Eric Boerwinkle<sup>10</sup>,  
7 Alanna C. Morrison<sup>10</sup>, Bruce M. Psaty<sup>13,14,15</sup>, Russell P. Tracy<sup>16,17</sup>, Susan R. Heckbert<sup>18</sup>, Michael  
8 H. Cho<sup>19,20</sup>, Jeong H Yun<sup>19,20</sup>, Nicholette D. Palmer<sup>21</sup>, Donald W. Bowden<sup>21</sup>, Joanne M.  
9 Murabito<sup>22,23</sup>, Daniel Levy<sup>24,25</sup>, Nancy L. Heard-Costa<sup>25,26</sup>, George T. O'Connor<sup>25,27</sup>, Lewis C.  
10 Becker<sup>28,29</sup>, Brian G. Kral<sup>28,29</sup>, Lisa R. Yanek<sup>29</sup>, Laura M. Raffield<sup>30</sup>, Bertha Hidalgo<sup>31</sup>, Jerome I.  
11 Rotter<sup>32</sup>, Stephen S. Rich<sup>33</sup>, Kent D. Taylor<sup>32</sup>, Wendy S. Post<sup>34</sup>, Charles Kooperberg<sup>35</sup>, Alexander  
12 P. Reiner<sup>18</sup>, Braxton D. Mitchell<sup>36</sup>, Sharon L.R. Kardinaal<sup>37</sup>, Jennifer A. Smith<sup>37</sup>, Patricia A. Peyser<sup>37</sup>,  
13 Lawrence F. Bielak<sup>37</sup>, Dong Keon Yon<sup>38,30,40,41,42</sup>, Hong-Hee Won<sup>43,44</sup>, Donna K. Arnett<sup>45</sup>, Albert  
14 V. Smith<sup>46</sup>, Stacey B. Gabriel<sup>47</sup>, Patrick T. Ellinor<sup>3,4,48,49</sup>, NHLBI Trans-Omics for Precision Medicine  
15 (TOPMed) Consortium, Pradeep Natarajan<sup>3,4,49,50,†</sup>, Minxian Wang<sup>1,2,5,51,52,53,†</sup>, Akl C.  
16 Fahed<sup>3,4,48,49,†</sup>

17 <sup>1</sup>National Genomics Data Center, China National Center for Bioinformation, Beijing, China, <sup>2</sup>Beijing Institute of  
18 Genomics, Chinese Academy of Sciences, Beijing, China, <sup>3</sup>Program in Medical and Population Genetics and the  
19 Cardiovascular Disease Initiative, Broad Institute of MIT and Harvard, Cambridge, MA, USA, <sup>4</sup>Cardiovascular  
20 Research Center, Massachusetts General Hospital, Boston, MA, USA, <sup>5</sup>College of Future Technology, Sino-  
21 Danish College, University of Chinese Academy of Sciences, Beijing, China., <sup>6</sup>Department of Medical Oncology,  
22 Dana-Farber Cancer Institute, Boston, MA, USA, <sup>7</sup>Division of Cardiovascular Medicine, Department of Medicine,  
23 Brigham and Women's Hospital, Boston, MA, USA, <sup>8</sup>Department of Vascular Medicine, Amsterdam Cardiovascular  
24 Sciences, Amsterdam University Medical Centers, Location AMC, University of Amsterdam, Amsterdam, the  
25 Netherlands, <sup>9</sup>Department of Internal Medicine, OLVG, Amsterdam, the Netherlands, <sup>10</sup>Human Genetics Center,  
26 Department of Epidemiology, School of Public Health, The University of Texas Health Science Center at Houston,  
27 Houston, TX, USA, <sup>11</sup>School of Public Health, University of Texas, San Antonio, TX, USA, <sup>12</sup>Department of  
28 Medicine, Boston University School of Medicine, Boston, MA, USA, <sup>13</sup>Cardiovascular Health Research Unit,  
29 Department of Medicine, University of Washington, Seattle, WA, USA, <sup>14</sup>Cardiovascular Health Research Unit,  
30 Department of Epidemiology, University of Washington, Seattle, WA, USA, <sup>15</sup>Cardiovascular Health Research Unit,  
31 Department of Health Systems and Population Health, University of Washington, Seattle, WA, USA, <sup>16</sup>Department  
32 of Pathology and Laboratory Medicine, The Robert Larner M.D. College of Medicine, University of Vermont,  
33 Burlington, VT, USA, <sup>17</sup>Department of Biochemistry, The Robert Larner M.D. College of Medicine, University of  
34 Vermont, Burlington, VT, USA, <sup>18</sup>Department of Epidemiology, University of Washington, Seattle, WA, USA,  
35 <sup>19</sup>Channing Division of Network Medicine, Brigham and Women's Hospital, Harvard Medical School, Boston, MA,  
36 USA, <sup>20</sup>Division of Pulmonary and Critical Care Medicine, Brigham and Women's Hospital, Harvard Medical School,  
37 Boston, MA, USA, <sup>21</sup>Department of Biochemistry, Wake Forest School of Medicine, 1 Medical Center Blvd,  
38 Winston-Salem, NC, USA, <sup>22</sup>Framingham Heart Study, National Heart, Lung, and Blood Institute and Boston  
39 University of Massachusetts Chan Medical School, Framingham, MA, USA, <sup>†</sup>Department of Medicine, Section

NOTE: This preprint reports new research that has not been certified by peer review and should not be used to guide clinical practice.

40 of General Internal Medicine, Boston University Chobanian & Avedisian School of Medicine and Boston Medical  
41 Center, Boston, MA, USA, <sup>24</sup>Population Sciences Branch, Division of Intramural Research National Heart, Lung,  
42 and Blood Institute, Framingham, MA USA, <sup>25</sup>Framingham Heart Study, Framingham, MA, USA, <sup>26</sup>Department of  
43 Neurology, Chobanian & Avedisian School of Medicine, Boston University, 72 E Concord St, Boston, MA, USA,  
44 <sup>27</sup>Boston University School of Medicine, Pulmonary Center, Boston, MA, USA, <sup>28</sup>Department of Medicine, Division  
45 of Cardiology, Johns Hopkins University School of Medicine, Baltimore, MD, USA, <sup>29</sup>Department of Medicine,  
46 Division of General Internal Medicine, GeneSTAR Research Program, Johns Hopkins University School of  
47 Medicine, Baltimore, MD, USA, <sup>30</sup>Department of Genetics, University of North Carolina, Chapel Hill, NC, USA,  
48 <sup>31</sup>Center for Clinical and Translational Science, The University of Alabama at Birmingham, Birmingham, AL, USA,  
49 <sup>32</sup>The Institute for Translational Genomics and Population Sciences, Department of Pediatrics, The Lundquist  
50 Institute for Biomedical Innovation at Harbor-UCLA Medical Center, Torrance, CA, USA, <sup>33</sup>Department of Genome  
51 Sciences, University of Virginia, Charlottesville, VA, USA, <sup>34</sup>Division of Cardiology, Department of Medicine, Johns  
52 Hopkins University, Baltimore, MD, USA, <sup>35</sup>Division of Public Health Sciences, Fred Hutchinson Cancer Center,  
53 Seattle, WA, USA, <sup>36</sup>Department of Medicine, University of Maryland School of Medicine, Baltimore, MD, USA,  
54 <sup>37</sup>Department of Epidemiology, School of Public Health, University of Michigan, Ann Arbor, MI, USA, <sup>38</sup>Center for  
55 Digital Health, Medical Science Research Institute, Kyung Hee University College of Medicine, Seoul, South Korea,  
56 <sup>39</sup>Department of Precision Medicine, Kyung Hee University College of Medicine, Seoul, South Korea,  
57 <sup>40</sup>Department of Regulatory Science, Kyung Hee University, Seoul, South Korea, <sup>41</sup>Department of Medicine,  
58 Kyung Hee University College of Medicine, Seoul, South Korea, <sup>42</sup>Department of Pediatrics, Kyung Hee University  
59 Medical Center, Kyung Hee University College of Medicine, Seoul, South Korea, <sup>43</sup>Department of Digital Health,  
60 Samsung Advanced Institute for Health Sciences & Technology (SAIHST), Sungkyunkwan University, Seoul, South  
61 Korea, <sup>44</sup>Samsung Genome Institute, Samsung Medical Center, Seoul, South Korea, <sup>45</sup>Office of the Provost,  
62 University of South Carolina, Columbia, SC, USA, Center for Statistical Genetics, <sup>46</sup>Department of Biostatistics,  
63 University of Michigan School of Public Health, Ann Arbor, MI, USA, <sup>47</sup>Broad Institute of MIT and Harvard,  
64 Cambridge, MA, USA, <sup>48</sup>Cardiology Division, Massachusetts General Hospital, Boston, MA, USA, <sup>49</sup>Harvard  
65 Medical School, Boston, MA, USA, <sup>50</sup>Center for Genomic Medicine, Massachusetts General Hospital, Boston, MA,  
66 USA, <sup>51</sup>Department of Cardiovascular Surgery, Zhongnan Hospital of Wuhan University, Wuhan, China, <sup>52</sup>Hubei  
67 Provincial Engineering Research Center of Minimally Invasive Cardiovascular Surgery, Wuhan, China, <sup>53</sup>Wuhan  
68 Clinical Research Center for Minimally Invasive Treatment of Structural Heart Disease, Wuhan, China.

69 **\*Contributed equally**

70 **† Jointly supervised this work**

71

72

73

74

75

76

77

78

79 **Please address correspondence to:**

80 Akl C. Fahed, MD, MPH

81 Cardiovascular Research Center, Massachusetts General Hospital, Boston, MA, USA

82 E-mail: [afahed@mgh.harvard.edu](mailto:afahed@mgh.harvard.edu)

83

84  
85 Minxian Wang, PhD

86 National Genomics Data Center, China National Center for Bioinformation, Beijing, China

87 E-mail: [wangmx@big.ac.cn](mailto:wangmx@big.ac.cn)

88

89

90

91

92

93

94

95

96

97

98

99

100

101

102

103

104

105

106

107

108

109

110

111

112

113 **Abstract**

114 Multiple germline and somatic genomic factors are associated with risk of coronary artery disease  
115 (CAD), but there is no single measure of risk that integrates all information from a DNA sample, limiting  
116 clinical use of genomic information. To address this gap, we developed an integrated genomic model  
117 (IGM), analogous to a clinical risk calculator that combines various clinical risk factors into a unified risk  
118 estimate. The IGM includes six genetic drivers for CAD, including germline factors (familial  
119 hypercholesterolemia [FH] variants, CAD polygenic risk score [PRS], proteome PRS, metabolome PRS)  
120 and somatic factors (clonal hematopoiesis of indeterminate potential [CHIP], and leukocyte telomere  
121 length [LTL]). We evaluated the IGM on CAD risk prediction in the UK Biobank (N=391,536), and  
122 validated it in the Trans-Omics for Precision Medicine (TOPMed) program (N=34,177). The 10-year  
123 CAD risk based on the IGM profile ranged from 1.1% to 15.5% in the UK Biobank and from 3.8% to  
124 33.0% in TOPMed, with a more pronounced gradient in males than females. IGM captured the  
125 cumulative effect of multiple genetic drivers, identifying individuals at high risk for CAD despite lacking  
126 obvious high risk genetic factors, or individuals at low risk for CAD despite having known genetic risk  
127 variants such as FH and CHIP. The IGM had the highest performance in younger individuals (C-statistic  
128 0.805 [95% CI, 0.699-0.913] for age  $\leq$  45 years). In middle age, IGM augmented the performance of  
129 the Pooled Cohort Equations (PCE), a clinical risk calculator for CAD. Adding IGM to PCE resulted in a  
130 continuous net reclassification index of 33.45% (95% CI, 32.11%-34.76%). We present the first model  
131 that integrates all currently available information from a single “DNA biopsy” to translate complex  
132 genetic information into a single risk estimate.

133

134

135

136

137

## 138 Introduction

139 The early identification of individuals at high risk for coronary artery disease (CAD) is a  
140 fundamental strategy in preventing disease which remains the number one cause of mortality and  
141 morbidity.<sup>1</sup> Utilizing DNA information for CAD risk prediction has gained traction due to its ability to  
142 identify early-onset cases, predict risk earlier in life, and augment the performance of existing clinical  
143 risk measures.<sup>2,3</sup> Significant progress has been made in understanding germline genomic risk drivers  
144 of CAD. Both monogenic drivers of risk such as pathogenic variants in familial hypercholesterolemia  
145 (FH)-related genes (*LDLR*, *APOB*, and *PCSK9*) and polygenic risk scores (PRS) have shown promise  
146 in CAD risk stratification, individually and in combination.<sup>4,5</sup> Moreover, age-related somatic mutations  
147 have been associated with increased CAD risk, attributed to clonal hematopoiesis of indeterminate  
148 potential (CHIP) and shortened leukocyte telomere length (LTL).<sup>6,7</sup> Even though germline and somatic  
149 genomic variations shape CAD risk, they remain to be studied in aggregate. A single model leveraging  
150 all available information from a single DNA biopsy could have the potential to improve risk prediction of  
151 CAD.

152 A comprehensive genomic risk model for CAD would integrate risk from early-life germline  
153 mutations with risk from somatic mutations occurring later in life. We previously demonstrated the  
154 interplay between monogenic and polygenic risk, highlighting that polygenic background alters the  
155 penetrance of FH variants.<sup>4</sup> Thereafter, Zhao et al. reported that a combination of germline and somatic  
156 mutations augments the risk of CAD, as evidenced by the interaction between PRS and CHIP.<sup>8</sup> This  
157 mounting evidence underscores that an ensemble model that integrates all known genetic drivers and  
158 their interactions might improve genomic risk prediction of CAD.

159 As genomic medicine moves towards clinical adoption, it might be beneficial that a single  
160 measure of risk is communicated using the entirety of the data points available from an individual's  
161 genome. Mixed information about risk is poised to confuse people unless integrated into a single  
162 number that is actionable. This concept has long been established in clinical risk prediction. For  
163 example, a single 10-year cardiovascular risk is provided by integrating information from factors such  
164 as blood pressure, cholesterol levels, smoking, and diabetes, each of which might indicate low or high  
165 risk for an individual.<sup>9</sup> Similarly, in genomic risk prediction, an individual might have a monogenic FH  
166 variant, a low polygenic risk score, no CHIP variant, and a short LTL, challenged by how to interpret  
167 this complex combination of genetic risk factors. It is only helpful for the individual in this context to  
168 understand the summed effect and risk estimate.

169 We developed an integrated genomic model (IGM) that uses a single score to maximize the  
170 precision in CAD risk prediction and enhance clinical translation. We demonstrated the accuracy,  
171 calibration, and added value of this all-at-once model using half a million people from the UK Biobank,  
172 and validated its performance in studies contributing to the Trans-Omics for Precision Medicine  
173 (TOPMed) program.

174

## 175 Results

### 176 Developing an Integrated Genomic Risk Model for CAD

177 We used the UK Biobank as a discovery cohort, including 391,536 individuals (mean [SD] age,  
178 56.5 [8.1] years; 53.8% women) including 28,346 (7.2%) participants who developed CAD over a  
179 median follow-up of 12.3 (interquartile range [IQR], 1.6) years. In the UK Biobank, 94.1% of participants  
180 were White (n = 368,296), with smaller proportions identifying as Asian (2.3%, n = 9,106), Black (1.6%,  
181 n = 6,237), and other ancestry (2.0%, n = 7,897). In contrast, TOPMed showed greater diversity, with  
182 68.3% White (n = 23,333), 25.9% Black (n = 8,858), 2.2% Asian (n = 737), and 3.7% Other ancestry (n  
183 = 1,250) (Supplementary Table 1). Whole-genome sequencing data was used to curate and compute  
184 features of risk previously shown to be associated with CAD. Specifically, we included two somatic  
185 features – CHIP and LTL– and four germline features – FH variants, CAD PRS, a proteome PRS  
186 (ProPRS) and a metabolome PRS (MetPRS). Of note, ProPRS and MetPRS were constructed using a  
187 series of genetic proxies for protein and metabolite levels derived from the atlas of genetic scores that  
188 predict multi-omics traits,<sup>10</sup> rather than relying on actual measurement of protein and metabolite levels.  
189 Using this feature matrix, we developed a somatic risk score, a germline risk score, and an integrated  
190 genomic model (IGM) (Fig. 1).

191 We then validated the IGM in 34,177 individuals from the TOPMed program (mean [SD] age,  
192 62.6 [10.6] years; 66.0% women) (Supplementary Table 1). Incident CAD events occurred in 3,972  
193 (14.3%) participants who developed CAD over a median follow-up of 10.5 (IQR, 8.6) years. The IGM  
194 model provided individual 10-year risk estimates across percentiles of somatic and germline risk (Fig.  
195 1). Further details on baseline characteristics by genetic drivers are presented in Supplementary Tables  
196 2-5.

### 197 Germline and Somatic Genomic Drivers of CAD Risk

198 We first estimated the individual risk of prevalent and incident CAD imparted by each of the two  
199 somatic and four germline drivers. When evaluating the association of the germline drivers with  
200 prevalent CAD in the UK Biobank, FH variant carriers had a three-fold increase in risk – odds ratio (OR)  
201 of 3.08 (95% confidence interval [CI], 2.46-3.85;  $p < 0.001$ ). The CAD PRS (OR per standard deviation  
202 (SD), 2.15; 95% CI, 2.11-2.19;  $p < 0.001$ ), MetPRS (OR per SD, 1.27; 95% CI, 1.25-1.29;  $p < 0.001$ ),  
203 and ProPRS (OR per SD, 1.19; 95% CI, 1.17-1.21;  $p < 0.001$ ) were also significantly associated with  
204 CAD (Fig. 2A). We combined these four germline risk factors into a single predictor called GermRisk.  
205 The OR per SD for GermRisk was 2.16 (95% CI, 2.12-2.20;  $p < 0.001$ ), and individuals in the top quintile  
206 of GermRisk had 3.6-fold increase in risk compared to everyone else (95% CI, 3.47-3.73;  $p < 0.001$ )  
207 (Supplementary Table 6). The effect sizes of genetic drivers for prevalent CAD in TOPMed were overall  
208 consistent with those of UK Biobank (Fig. 2B; Supplementary Table 7).

209 We then evaluated the association of genomic drivers with incident CAD in the UK Biobank,  
210 and demonstrated strong associations of each of the germline and somatic drivers with incident CAD  
211 (Fig. 2C; Supplementary Table 8). For germline drivers, the HR for FH carriers was 1.69 (95% CI 1.41-  
212 2.03,  $p < 0.001$ ) and HRs per SD for CAD PRS, MetPRS, and ProPRS were 1.56 (95% CI 1.55-1.58,  $p$   
213  $< 0.001$ ), 1.18 (95% CI 1.17-1.19,  $p < 0.001$ ), and 1.15 (95% CI 1.14-1.17,  $p < 0.001$ ), respectively. For  
214 somatic drivers, CHIP and LTL were associated with CAD with HR of 1.13 (95% CI 1.06-1.20,  $p < 0.001$ )  
215 and 0.94 (95% CI 0.92-0.95,  $p < 0.001$ ), respectively. We combined these two somatic risk factors into  
216 a single predictor called SomaRisk, similar to GermRisk. Both GermRisk and SomaRisk demonstrated  
217 a strong association with incident CAD – HR per SD of 1.57 (95% CI 1.55-1.59,  $p < 0.001$ ) and 1.05  
218 (95% CI 1.04-1.06,  $p < 0.001$ ), respectively (Fig. 2C; Supplementary Table 8). The effect sizes of  
219 genetic drivers for incident CAD in TOPMed were mostly consistent with those of UK Biobank (Fig. 2D;  
220 Supplementary Table 9).

### 221 Integrated Genomic Model to Predict CAD Risk



222 We assessed pairwise correlations between six genetic variables from the UK Biobank and  
223 TOPMed studies using Pearson correlation coefficients to evaluate multicollinearity before combining  
224 them in a Cox proportional hazards model. This allowed us to gauge overlapping signals, particularly  
225 between CAD PRS, MetPRS, and ProPRS. The correlations among six drivers were weak ( $\leq 0.3$ ) (Fig.  
226 2E and 2F), reassuring that each driver contributes distinct signals.

227 To obtain a comprehensive assessment of a person's CAD risk, we used an integrated genomic  
228 model (IGM) to quantify the risk from both germline and somatic drivers – a combined predictor of  
229 GermRisk and SomaRisk (Supplementary Fig. 1). The IGM risk was significantly associated with the  
230 risk of incident CAD (HR per SD, 1.58; 95% CI, 1.56-1.59;  $p < 0.001$ ), and the effect size was consistent  
231 when validated in the TOPMed external data set (HR per SD, 1.46; 95% CI, 1.40-1.53;  $p < 0.001$ ) (Fig.  
232 2C and 2D; Supplementary Tables 8-9).

233 Joint modeling of germline and somatic drivers indicated substantial gradients in risk of CAD,  
234 according to inherited DNA variants and variation in the rate of LTL shortening and accumulation of  
235 somatic variants leading to CHIP. For the sex-combined estimation of the 10-year risk of CAD in UK  
236 Biobank, individuals in the lowest germline and somatic risk percentile have a 10-year risk as low as  
237 1.1%, while those in the highest germline and somatic risk percentile have a 10-year risk as high as  
238 15.5% (Fig. 3A). A similar gradient in risk across germline and somatic variation was observed in  
239 TOPMed, ranging from 3.8% to 33.0% (Fig. 3B). For a sex-stratified analysis in the UK Biobank, male  
240 individuals had a 10-year risk that ranged from 1.8% to 23.0% across the germline and somatic risk  
241 spectrum. This was about 2.3 times higher than the risk spectrum for females, which spanned from 0.7%  
242 to 10.3% (Fig. 3C). Large gradients in 10-year risk were consistently observed in the TOPMed for the  
243 sex-stratified analysis, with males ranging from 4.8% to 39.9% and females ranging from 3.0% and  
244 27.0% (Fig. 3D).

#### 245 **Heterogeneity of Genomic Risk Profiles Captured by the Integrated Genomic Model**

246 The IGM effectively captured a range of genetic risk combinations for CAD, identifying high risk  
247 groups (top 20% overall risk) with diverse genetic profiles in the UK Biobank (Fig. 4A). High risk IGM  
248 group included individuals at high risk in both germline and somatic factors (20.6%), those at high risk  
249 for one of the factors (78.6%), and a small proportion with moderately elevated, yet sub-threshold, risks  
250 for both factors (0.8%) (Fig. 4A). Individuals at high risk for both germline and somatic factors had the  
251 highest 10-year risk (8.8%, 95% CI 8.43-9.19%) within the high risk IGM group (Supplementary Table  
252 10). As expected, the high risk group identified by the IGM had a larger number of genetic risk drivers  
253 compared to the low risk group. For example, 63.9% had two or more genetic drivers in the high risk  
254 group, compared to only 3.4% in the low risk group in the UK Biobank (Fig. 4B). Notably, people at low  
255 IGM risk were not without genetic risk drivers, and a non-negligible proportion of 29.3% had one or  
256 more genetic risk drivers (Fig. 4B and Supplementary Table 11); however, mitigating effects from other  
257 genetic variants (e.g., low CAD PRS) seem to offset the overall risk, thus classifying these individuals  
258 as low risk. Similar proportions of breakdown and distribution patterns were observed in TOPMed (Fig.  
259 4C, 4D and Supplementary Table 11).

#### 260 **Integrated Genomic Model and Clinical Risk**

261 The American College of Cardiology/American Heart Association, Pooled Cohort Equations  
262 (PCE) are a guideline-recommended clinical-risk calculator that uses clinical risk factors to identify high  
263 risk people for initiation of preventive treatments (i.e., statin).<sup>11</sup> Within each of the guideline-defined  
264 strata of the PCE risk, the IGM score was a strong predictor of coronary artery disease events and  
265 showed a consistent risk gradient by IGM score category (Fig. 5A, B). Among participants at high PCE  
266 risk ( $> 20\%$  10-year risk), the 10-year CAD event rates were 5.4%, 9.5%, and 16.4%, for low,  
267 intermediate, and high IGM risk groups (Fig. 5A). Remarkably, a 10-year CAD risk threshold of 7.5%  
268 for initiating statin therapy as guideline recommended was reached even among individuals in the  
269 borderline (5.0%-7.4% 10-year risk) and intermediate (7.5%-19.9% 10-year risk) PCE categories when

270 stratified by IGM percentiles (Fig. 5B) – an IGM score higher than 95th and 72nd percentile, respectively  
271 for borderline and intermediate risk (Fig. 5B). A close match of the model predicted and actual observed  
272 10-year disease risk shows the models were well calibrated (Supplementary Fig. 2). When  
273 disaggregated to individual genetic risk drivers, the FH variants and CAD PRS most prominently re-  
274 stratified the CAD risk across PCE categories, but other risk factors also have significant stratification  
275 ability (Supplementary Fig. 3).

276 By combining the conventional clinical risk of PCE with the genetic risk of IGM, the model  
277 showed the most potent risk stratification ability. When 20,624 individuals who experienced CAD events  
278 in the UK Biobank were used to determine reclassification by adding IGM to PCE compared to PCE  
279 alone, 1,858 were correctly classified at a higher risk, while 1,452 were incorrectly placed at a lower  
280 risk (Fig. 5C), leading to a net proportion of accurate reclassifications for events is 1.97% (406/20,624).  
281 For nonevents, 22,954 individuals were correctly down-classified, and 16,708 were incorrectly up-  
282 classified, leading to a net reclassification proportion of 1.75% (6,246/356,656) for nonevents. The  
283 overall NRI combines the events and nonevents, resulting in 3.72% (95% CI, 3.15%-4.26%).  
284 Continuous NRI was 33.45% (95% CI, 32.11%-34.76%). As shown in the full stratification table, there  
285 was a lower event rate in the low risk category for the combined model than in the PCE-alone model  
286 (1.9% versus 2.3%), however, a higher event rate was observed for the high risk category (27.1%  
287 versus 23.5%), demonstrating the prominent risk stratification ability of the IGM model with guideline-  
288 recommended PCE risk estimator (Supplementary Table 12).

289 Finally, we evaluated the discrimination of PCE, IGM, and combined model compared to a  
290 baseline model with age, sex and genetic ancestry. The C-statistic for the base model was 0.701 (95%  
291 CI, 0.698-0.704), PCE was 0.725 (95% CI 0.722-0.728), and the combination of base and IGM model  
292 was 0.734 (95% CI 0.731–0.737), respectively, in UK Biobank (Supplementary Fig. 4A; Supplementary  
293 Table 13). The performance was highest when combining PCE and IGM (C-statistic, 0.750; 95% CI,  
294 0.747-0.753). In the TOPMed data, the discrimination with IGM was further improved when limiting  
295 prediction to younger individuals (aged  $\leq$  45 years) (C-statistic 0.805, 95% CI, 0.699-  
296 0.913)( Supplementary Fig. 4B and Supplementary Table 13).

297

298



## 299 Discussion

300 We developed an integrated genomic model for CAD prediction that combines multiple known  
301 germline and somatic risk drivers that can be measured using a single DNA biopsy. The model  
302 demonstrated value in improving the precision of risk estimation and capturing people at risk due to  
303 diverse genetic risk profiles. Based on the IGM, the 10-year CAD risk varied from 1.1% to 15.5% among  
304 UK Biobank participants and 3.8% to 33.0% in TOPMed study participants, with a more pronounced  
305 gradient in males than females for both cohorts. The integrated genomic score showed a high  
306 discrimination when combined with clinical risk score or used in younger age groups. The addition of  
307 the IGM to the clinical risk model resulted in a continuous net reclassification index of 33.45%. The  
308 integrated genomic model captured cumulative and comprehensive effects of multiple genetic drivers,  
309 identifying high risk individuals who may otherwise be overlooked when using conventional risk models  
310 relying on a single genomic driver (i.e., PRS or FH).

311 Conventional genomic risk models for CAD that focused on monogenic (FH) or polygenic (PRS)  
312 drivers were limited in their uniaxial approach, falling short of encompassing the wide range of genetic  
313 combinations present in real-world populations.<sup>12</sup> For instance, individuals carrying FH and CHIP  
314 variants might still have a low overall risk of CAD if their effects are offset by protective PRS and low  
315 MetPRS. Other individuals may present with different combinations of risk and protective genetic factors  
316 that collectively indicate a high CAD risk. Such dynamics complicate CAD risk assessment using  
317 standard genomic approaches that rely on stratification by a single genetic driver. Our IGM captured  
318 such dynamics by integrating all known genomic risk drivers for CAD, including germline, somatic, and  
319 predicted proteomic/metabolomic drivers in a single model, without compromising the performance. We  
320 successfully demonstrated that IGM captures cumulative and comprehensive effects of multiple genetic  
321 drivers, identifying high risk individuals who do not have obvious germline and somatic risk but whose  
322 aggregate genetic risk escalates to a high overall risk (Fig. 4A, 4B). Conversely, a subset of individuals  
323 classified in the low risk group by IGM possessed one or more high risk genetic drivers (Fig. 4C),  
324 indicating other drivers may confer protective benefits and thus reduce the overall risk. Such a dynamic  
325 profile of personal genomics should be considered to fully achieve the goals of precision prevention and  
326 personalized care.

327 The high risk group identified by the IGM exhibited an impressive diversity in their genetic  
328 profiles and combinations. In the high risk group identified by IGM, 20.9% and 19.8% of individuals  
329 carried a high risk classification for more than 3 genetic drivers while 36.1% and 37.6% had a high risk  
330 for only 1 or 0 drivers in UK Biobank and TOPMed studies, respectively (Supplementary Table 11).  
331 Interestingly, in the low risk group by IGM (bottom 20%), there were 32 and 593 UK Biobank participants  
332 carrying FH and CHIP variants respectively, suggesting that a single genetic factor does not necessarily  
333 dictate the overall risk for the disease (Supplementary Table 14). Our observation unveiled a cumulative  
334 pattern where the protective level of one or a group of drivers can offset the risk posed by others. The  
335 multidimensional nature of our model might facilitate a nuanced approach to risk stratification and draw  
336 clinical attention to at-risk individuals who would have otherwise been overlooked by conventional  
337 genomic models that are not designed to capture diversity of the genetic pool.

338 The integrated genomic model based on comprehensive DNA information is a strong predictor  
339 of CAD in young adults enabling primordial prevention prior to the onset of clinical risk factors. While  
340 IGM had modestly higher discriminative capacity for incident CAD compared with the clinical risk score,  
341 its predictive accuracy was significantly higher in younger individuals (aged  $\leq 45$  years) in the TOPMed  
342 program studies (C-statistic 0.805) (Supplementary Table 13). Our findings imply that the use of genetic  
343 information to predict future CAD risk might be more profound for young adults, consistent with previous  
344 findings.<sup>13,14</sup> In contrast to clinical risk models, the IGM is available even before clinical risk factors  
345 manifest, providing an additional benefit to young adults who often remain undetected on the radar of  
346 traditional assessments.

347 The highest prediction was achieved by combining IGM with clinical risk score, highlighting the  
348 value of genetics in complementing clinical risk prediction. The IGM enabled risk stratification for CAD  
349 within each clinical risk stratum, enhancing the identification of individuals requiring targeted clinical  
350 interventions. Low genetic risk individuals in the high PCE group demonstrated equivalent 10-year CAD  
351 risk with average genetic risk individuals in the intermediate PCE group, and a consistent downward  
352 trend was observed across all clinical risk strata (Fig. 5A). Conversely, an upward trend was observed  
353 for individuals with high genetic risk identified by IGM. Current guidelines recommend initiating statin  
354 therapy for individuals in the intermediate PCE category, defined as a 10-year CAD risk of 7.5% or  
355 higher.<sup>15</sup> However, our findings indicate that individuals in the borderline PCE category who have a high  
356 genetic risk may also warrant targeted interventions, as their 10-year CAD risk is comparable (Fig. 5A).  
357 It is noteworthy that individuals at the 33rd, 72nd, and 95th percentiles of integrated genomic risk all  
358 exhibited an equivalent 10-year CAD risk of 7.5% (Fig. 5B), despite being categorized in high,  
359 intermediate, and borderline PCE groups, respectively. This further indicated that existing clinical-  
360 focused models might not adequately encompass the multifaceted nature of CAD risk, warranting the  
361 consideration of the interplay between genetic and clinical factors in risk evaluations.

362 While monogenic and polygenic drivers of risk have become well-established, emerging models  
363 based on proteomic data are now being developed to predict cardiovascular risk, expanding beyond  
364 traditional clinical and genomic models.<sup>16,17</sup> Helgason et al. recently developed a protein risk score  
365 based on 4,963 plasma proteins from 13,540 Icelanders and demonstrated reliable predictability for  
366 major cardiovascular risk.<sup>16</sup> Nevertheless, implementation of proteome measurement in clinical practice  
367 remains challenging due to the cost and feasibility constraints. To make the most of proteomic and  
368 metabolomic insights in settings without their direct measurements, we developed proteome and  
369 metabolome PRSs, leveraging genetically-predicted protein and metabolite levels instead of actual  
370 serum protein levels based on the genetic score atlas for multi-omics traits.<sup>10</sup> We calculated genetic  
371 score for 2,692 proteins and 876 metabolites levels, with 124 proteins and 142 metabolites comprising  
372 the final ProPRS and MetPRS models after Lasso penalty was applied, respectively (Supplementary  
373 Fig. 5; Supplementary Tables 15-16). Although some correlation was present among the MetPRS,  
374 ProPRS and CAD PRS, the magnitude was weak ( $\leq 0.3$ ) (Fig. 2), implicating that each driver  
375 contributes a distinct, non-overlapping signal. To the best of our knowledge, we have introduced the  
376 first genetically-predicted protein and metabolite risk scores for CAD risk prediction, which are readily  
377 obtainable through standard low-cost DNA microarray or sequencing and thereby more cost-effective  
378 than serum protein measurements. Our purpose was to make the most out of a single DNA biopsy,  
379 which is becoming increasingly feasible through adoption of genomic medicine and large biobanking  
380 efforts.

381 This study has several limitations. First, we have not provided ancestry-specific results given  
382 the majority composition with European and smaller sample size for non-European ancestries. However,  
383 to promote inclusion and equity, we used multi-ancestry cohorts from UK Biobank and TOPMed in the  
384 primary analysis, as well as multi-ancestry PRS that has been demonstrated to perform well for both  
385 European and non-European ancestries.<sup>12</sup> Second, this study evaluated CAD as the primary outcome  
386 whereas PCE was developed to predict cardiovascular disease which includes CAD and stroke.  
387 Nevertheless, previous studies have shown that the PCE is effective in predicting CAD.<sup>18,19</sup> Third, the  
388 CAD PRS used in this study included low frequency and common variants, but did not incorporate rare  
389 high-impact genetic variants associated with CAD risk. However, based on whole genome sequencing  
390 data from half a million populations, we separately identified somatic mutations and curated significant  
391 rare variants such as those linked to FH to develop a comprehensive genomic model. This approach  
392 allowed us to comprehensively capture the diverse spectrum of genetic variant frequencies linked to  
393 CAD. Fourth, baseline CAD risk is different in the UK Biobank and TOPMed because UK Biobank  
394 consists of healthier individuals compared to TOPMed. The incidence of CAD was 7.2% and 12.7%  
395 respectively for UK Biobank and TOPMed (Supplementary Table 1), and this was reflected in the risk  
396 gradient captured by IGM the 10-year CAD risk ranged from 1.1% to 15.5% among UK Biobank

397 participants, and 3.8% to 33.0% in TOPMed participants (Fig. 3).

## 398 **Conclusion**

399 We integrated all currently available information from a single “DNA biopsy” to translate complex genetic  
400 information into a single risk estimate. The IGM powerfully stratifies CAD risk in young individuals and  
401 complements clinical risk prediction in middle-aged individuals. Because the model considered the  
402 contributions of multiple genomic drivers for every individual, it was able to identify high risk individuals  
403 who may otherwise be overlooked when using conventional risk models relying on a single genomic  
404 driver. Our model holds the promise to transform CAD risk assessment strategies in an emerging  
405 'genome-first' healthcare framework, where genomic information becomes readily accessible and a  
406 fundamental part of patient care. Moreover, the framework we propose could be extended to other  
407 diseases known to have multiple genomic risk drivers.

## 408 **Methods**

### 409 **Dataset and Quality Control**

410 Access to the UK Biobank data was approved with application ID 89885. Samples with discordance  
411 between self-reported sex (Field 31) and genetically inferred sex (Field 22001) were removed.  
412 Additionally, samples with individual-level genotype missing rates (Field 22005) greater than 5%,  
413 outliers for heterozygosity or missing rate (Field 22027), or sex chromosome aneuploidy (Field 22019)  
414 were excluded. To remove close relatives in the samples, we excluded one of the samples whose  
415 pairwise kinship value is greater than or equal to 0.0884 (threshold of the second-degree close  
416 relatives<sup>20</sup>) but also tried to keep as many samples as possible. Finally, 391,536 individuals were  
417 included in the final analysis (Supplementary Fig. 6A).

418 A total of 80,588 participants from the NHLBI's TOPMed program with available whole genome  
419 sequencing data were considered. These studies primarily consist of observational cohorts that have  
420 been described in detail previously.<sup>6</sup> Among 80,588 participants, we excluded 49 samples with  
421 conflicting sex information, 1 sample without principal components, and 17,237 samples with excess  
422 kinship, defined as a second-degree relationship or closer, indicated by a KING coefficient greater than  
423 0.0884. Finally, 34,177 participants remained for analysis after excluding an additional 29,124  
424 participants without CAD phenotype (Supplementary Fig. 6B). Cohorts contributed to this population  
425 are Amish, Atherosclerosis Risk in Communities Study[ARIC], Cardiovascular Health Study[CHS],  
426 Genetic epidemiology of COPD[COPDGene], Diabetes Heart Study[DHS], Framingham Heart  
427 Study[FHS], Genetic Study of Atherosclerosis Risk[GeneSTAR], Genetic Epidemiology Network of  
428 Arteriopathy[GENOA], Jackson Heart Study[JHS], Multi-Ethnic Study of Atherosclerosis[MESA], and  
429 Women's Health Initiative[WHI].

### 430 **Curation of FH, CHIP, and LTL**

431 To determine the carrier status of familial hypercholesterolemia (FH) for samples with available whole-  
432 exome sequencing data, a combination of variant selection criteria was applied: 1) Variants from  
433 previous publications which were manually curated by clinical geneticists;<sup>4,21–23</sup> 2) Variants in *LDLR*,  
434 *APOB* and *PCSK9* from the ClinVar database (downloaded February 27th, 2023, GRCh38) annotated  
435 as pathogenic, likely pathogenic, or pathogenic/likely pathogenic without conflicts. For *APOB* and  
436 *PCSK9* gene, only variants associated with hypercholesterolemia but not hypobetalipoproteinemia were  
437 included; 3) Variants in *LDLR* annotated as high-confidence loss-of-function by the VEP Loss-Of-  
438 Function Transcript Effect Estimator (LOFTEE) plugin were also included.<sup>24,25</sup> Only variants with a net  
439 positive association with LDL cholesterol level accessed by an iterative conditional regression analysis  
440 were included in the final variant list for subsequent analysis (Supplementary Table 17).<sup>26</sup>

441 The carrier status of clonal hematopoiesis of indeterminate potential (CHIP) was detected following a  
442 similar procedure described in Yu Zhi et al. and others.<sup>27–29</sup> Specifically, carrier status was determined  
443 by carrying CHIP variants from one of the genes *TET2*, *ASXL1*, *JAK2*, *PPM1D*, *TP53*, *SRSF2*, and  
444 *SF3B1*. Leukocyte telomere length (LTL) was log-transformed to obtain a normal distribution and then  
445 Z-standardized using the distribution of all individuals with a telomere length measurement (Field  
446 22192). Details of processing were described in V. Codd et al.<sup>30</sup> Unless otherwise specified, genetic  
447 drivers have been curated comparably for UK Biobank and TOPMed. More details on the curation of  
448 CHIP and LTL for TOPMed are described elsewhere.<sup>6</sup>

### 449 **CAD Polygenic Risk Score, Metabolome Polygenic Risk Score, and Proteome Polygenic Risk Score**

451 In the UK Biobank, CAD PRS was calculated using the imputed genotype data and variant weights from

452 the multi-ancestry and multi-trait polygenic risk score for CAD described in A. P. Patel et al.,<sup>12</sup>  
453 implemented with PLINK2.<sup>31</sup> Proxy Risk scores for Metabolome (Metabolon and Nightingale) and  
454 Proteome (Somalogic and Olink) were calculated with the imputed genotype data and model weight  
455 files downloaded from OMICS PRED resource which derived from the INTERVAL study cohort  
456 (<https://www.omicspred.org/Scores/Somalogic/INTERVAL>),<sup>10</sup> with 726 (Metabolon), 141 (Nightingale),  
457 2,384 (Somalogic), and 308 (Olink) scores, respectively. We randomly sampled 200,000 individuals  
458 from UK Biobank as the training set, and a lasso penalty was applied to the Cox proportional hazards  
459 regression model with age, sex, and the top 10 principal components (PCs) as covariates and incident  
460 CAD as an outcome, similar to the process described elsewhere.<sup>16</sup> Five-fold cross-validation was  
461 employed to select the optimal penalization strength for hyperparameters. Two independent models  
462 were trained for the prediction of CAD risk using proxy scores of metabolome (genetic risk scores for  
463 867 serum metabolites) and proteome (genetic risk scores for 2,692 serum proteins). With weights  
464 determined by the cross-validation procedures, the weighted proxy risk scores for Metabolome  
465 (MetPRS) and Proteome (ProPRS) were then calculated for all samples. The number of genetically  
466 predicted metabolome and proteome scores retained in the MetPRS and ProPRS lasso models were  
467 142 and 124, respectively (Supplementary Tables 15-16).

## 468 **CAD Definition**

469 In the UK Biobank, CAD was defined based on self-report at enrollment, hospitalization records, or  
470 death registry records as previously described (Supplementary Table 18).<sup>4</sup> In the TOPMed studies,  
471 CAD was defined as ischemic heart disease events, including myocardial infarction and coronary  
472 revascularization.<sup>6</sup> Incident CAD cases were defined as those diagnosed after recruitment. The survival  
473 year was defined as the years between recruitment and diagnosis for incident CAD cases, or between  
474 the time of the recruitment and the last censoring for controls.

## 475 **Covariates and Adjustment**

476 Untreated blood pressure was estimated by adjusting the raw value for anti-hypertensive medication  
477 intake by adding 15 mmHg to the systolic blood pressure and 10 mmHg to the diastolic blood pressure  
478 as previously described.<sup>32,33</sup> Untreated lipid levels were estimated by adjusting the raw lab-tested value  
479 according to lipid-lowering medication intake as described previously<sup>12</sup> and detailed in Supplementary  
480 Table 19.

481 To eliminate potential confounding effects of covariates, PRS, MetPRS, ProPRS, and LTL were  
482 regressed on recruitment age, sex, and the first 10 principal components of genetic ancestry  
483 (Supplementary Fig. 7). The scaled residuals with mean zero and standard deviation of one were then  
484 used in the subsequent analyses.

## 485 **Developing the integrated genomic risk model**

486 We evaluated pairwise correlations between six genetic variables from the UK Biobank and TOPMed  
487 studies to assess potential multicollinearity before including these variables in a regression model. The  
488 correlation matrix was computed using Pearson correlation coefficients. As germline genetic risk drivers  
489 (FH, PRS, MetPRS, and ProPRS) remain constant from birth, while CHIP accumulates and LTL  
490 shortens with age (somatic risk drivers), we systematically characterized and investigated the joint  
491 effects of germline and somatic risk drivers on CAD. Germline risks were combined into a single value  
492 termed GermRisk, and somatic risks were combined into a single value termed SomaRisk, the  
493 combination weights were estimated by a joint regression model. Specifically, for prevalent CAD, the  
494 germline risk drivers (FH, PRS, MetPRS, and ProPRS) were fitted into a logistic regression model, and  
495 the coefficients were used as weights to combine the values of the drivers into GermRisk linearly. For  
496 incident CAD, the germline risk drivers were fitted to a Cox proportional hazards model, and GermRisk



497 was calculated as a weighted summation of germline variables and their corresponding Cox coefficients,  
498 and similar procedures were performed to obtain SomaRisk.

499 Next, GermRisk and SomaRisk were regressed on recruitment age, sex, and the top 10 PCs, and the  
500 residuals were scaled to have zero mean and unit standard deviation, respectively. The standardized  
501 residuals of GermRisk and SomaRisk were then fitted to a Cox proportional hazards model. A final  
502 predictor, termed IGM (integrated genomic model), was a linear summation of GermRisk and SomaRisk  
503 residual according to the Cox coefficient estimation. The weights were fixed and applied to TOPMed  
504 data for independent validation. The overall framework for developing and validating the integrated  
505 genomic model is shown in Fig. 1.

## 506 **Estimating Effect Sizes**

507 To investigate the genomic factors driving the risk of prevalent and incident CAD, a logistic regression  
508 model and Cox proportional hazards regression model were employed respectively to estimate the  
509 effect sizes for individual genetic drivers. Additionally, PRS, MetPRS, ProPRS, LTL, and the ensembled  
510 ones (IGMRisk, GermRisk and SomaRisk) were binarized, with individuals in the top 20% treated as  
511 carriers (hPRS, hMetPRS, hProPRS, hIGMRisk, hGermRisk and hSomaRisk) or bottom 20% treated  
512 as a carrier (sLTL) for telomere length.

## 513 **Interplay Between Genomic Drivers and Clinical Risk Score**

514 To investigate the interplay between genomic risk and PCE, participants in the UK Biobank were divided  
515 into four groups based on guideline-defined categories of the PCE – low (estimated risk less than 5%),  
516 borderline (risk between 5% to 7.5%), intermediate (risk between 7.5% and 20%), and high (risk greater  
517 than 20%).<sup>15</sup> For the IGM, we divide samples into three risk groups as standard in genomic analyses –  
518 high genomic risk (top quintile of the distribution), intermediate genomic risk (middle three quintiles),  
519 and low risk (bottom quintile).

## 520 **Estimating 10-year risk of CAD**

521 The 10-year risk of CAD was estimated by Cox proportional hazards regression with GermRisk and  
522 SomaRisk as predictors and the age, sex, and first 10 principal components of genetic ancestry as  
523 covariates. To investigate the stratification capacity of different models, the C-statistic from 1) a base  
524 model (sex, age, and first 10 PCs), 2) a log-transformed value of PCE, 3) a base model and IGM, and  
525 4) a base model, IGM and log(PCE), was estimated by a Cox proportional hazards model, respectively.

526 To evaluate the improvement of prediction by adding the IGM to PCE, the net reclassification  
527 improvement was calculated based on a 10-year risk threshold of 7.5% for categorical reclassification  
528 and threshold 0 for continuous reclassification as demonstrated elsewhere.<sup>18,19</sup> Confidence intervals  
529 were estimated by 100 times bootstrap. All statistical analyses were done using R v4.2.2 (R Foundation,  
530 Vienna, Austria), including the following packages: survival (v3.5-7), survminer (v0.4.9), tableone  
531 (v0.13.2), pROC(v1.18.5), nricens(v1.6), rms(v6.7-1) and glmnet (v4.1-8).

## 532 **Data availability**

533 All data are made available from the UK Biobank (<https://www.ukbiobank.ac.uk/enable-your-research/apply-for-access>) to researchers from universities and other institutions with genuine  
534 research inquiries following institutional review board and UK Biobank approval. This research was  
535 conducted using the UK Biobank resource under Application Number 89885 and approved by Beijing  
536 Institute of Genomics review board. The weights of MetPRS and ProPRS are available in the  
537 Polygenic Score Catalog (IDs: PGS005093-PGS005094). This paper used the TOPMed whole  
538 genome sequencing (WGS) data and cardiovascular disease phenotype data. Genotype and  
539 phenotype data are both available in database of Genotypes and Phenotypes (dbGaP). The TOPMed  
540



541 WGS data were from the following eleven study cohorts: Amish, Atherosclerosis Risk in Communities  
542 Study (ARIC), Cardiovascular Health Study (CHS), Genetic epidemiology of COPD (COPDGene),  
543 Diabetes Heart Study (DHS), Framingham Heart Study (FHS), Genetic Study of Atherosclerosis Risk  
544 (GeneSTAR), Genetic Epidemiology Network of Arteriopathy (GENOA), Jackson Heart Study (JHS),  
545 Multi-Ethnic Study of Atherosclerosis (MESA), and Women's Health Initiative (WHI).

## 546 Acknowledgements

547  
548 Dr. Ellinor is supported by grants from the National Institutes of Health (R01HL092577, 1R01HL157635,  
549 5R01HL139731), from the American Heart Association (18SFRN34110082, 961045) and from the  
550 European Union (MAESTRIA 965286). Dr. Natarajan is funded by grants R01HL1427, R01HL148565  
551 R01HL148050, and U01HG011719 from the National Institutes of Health. Dr. Fahed is funded by grants  
552 K08HL161448 and R01HL164629 from the National Institutes of Health. Dr. de Vries is funded by  
553 R01HL146860 from the National Heart, Lung and Blood Institute (NHLBI). Dr. Wang is supported by  
554 the Pioneering Action Grants of the Chinese Academy of Sciences. Molecular data for the Trans Omics  
555 in Precision Medicine (TOPMed) program was supported by the NHLBI. Core support including  
556 centralized genomic read mapping and genotype calling, along with variant quality metrics and filtering  
557 were provided by the TOPMed Informatics Research Center (3R01HL-117626-02S1; contract  
558 HHSN268201800002I). Core support including phenotype harmonization, data management, sample-  
559 identity QC and general program coordination was provided by the TOPMed Data Coordinating Center  
560 (R01HL-120393; U01HL-120393; contract HHSN268201800001I). We gratefully acknowledge the  
561 studies and participants who provided biological samples and data for TOPMed. The views expressed  
562 in this manuscript are those of the authors and do not necessarily represent the views of the National  
563 Heart, Lung, and Blood Institute, the National Institutes of Health, or the U.S. Department of Health and  
564 Human Services. We wish to acknowledge the contributions of the consortium working on the  
565 development of the NHLBI BioData Catalyst ecosystem. Support for the Genetic Epidemiology Network  
566 of Arteriopathy (GENOA) was provided by the National Heart, Lung and Blood Institute (U01 HL054457,  
567 U01 HL054464, U01 HL054481, R01 HL119443, and R01 HL087660) of the National Institutes of  
568 Health. DNA extraction for “NHLBI TOPMed: Genetic Epidemiology Network of Arteriopathy”  
569 (phs001345) was performed at the Mayo Clinic Genotyping Core, and WGS was performed at the DNA  
570 Sequencing and Gene Analysis Center at the University of Washington (3R01HL055673-18S1) and the  
571 Broad Institute (HHSN268201500014C). We would like to thank the GENOA participants. The Jackson  
572 Heart Study (JHS) is supported and conducted in collaboration with Jackson State University  
573 (HHSN268201800013I), Tougaloo College (HHSN268201800014I), the Mississippi State Department  
574 of Health (HHSN268201800015I) and the University of Mississippi Medical Center  
575 (HHSN268201800010I, HHSN268201800011I and HHSN268201800012I) contracts from the NHLBI  
576 and the National Institute on Minority Health and Health Disparities (NIMHD). Genome sequencing for  
577 “NHLBI TOPMed: The Jackson Heart Study” (phs000964.v1.p1) was performed at the Northwest  
578 Genomics Center (HHSN268201100037C). The authors also wish to thank the staffs and participants  
579 of the JHS. The MESA projects are conducted and supported by NHLBI in collaboration with MESA  
580 investigators. Support for the Multi-Ethnic Study of Atherosclerosis (MESA) projects are conducted and  
581 supported by the NHLBI in collaboration with MESA investigators. Support for MESA is provided by  
582 contracts 75N92020D00001, HHSN268201500003I, N01-HC-95159, 75N92020D00005, N01-HC-  
583 95160, 75N92020D00002, N01-HC-95161, 75N92020D00003, N01-HC-95162, 75N92020D00006,  
584 N01-HC-95163, 75N92020D00004, N01-HC-95164, 75N92020D00007, N01-HC-95165, N01-HC-  
585 95166, N01-HC-95167, N01-HC-95168, N01-HC-95169, UL1-TR-000040, UL1-TR-001079, UL1-TR-  
586 001420, UL1TR001881, DK063491, R01HL105756, and R01HL146860. Genome sequencing for  
587 “NHLBI TOPMed: Whole Genome Sequencing and Related Phenotypes in the Multi-Ethnic Study of  
588 Atherosclerosis Study (MESA)” (phs001416) was performed at Broad Institute of MIT and Harvard  
589 Genomics Platform (3U54HG003067-13S1). The authors thank the other investigators, the staff, and  
590 the participants of the MESA study for their valuable contributions. A full list of participating MESA  
591 investigators and institutes can be found at <http://www.mesa-nhlbi.org>. The Women’s Health Initiative  
592 (WHI) program is funded by the National Heart, Lung, and Blood Institute, National Institutes of Health,  
593 U.S. Department of Health and Human Services through contracts 75N92021D00001,  
594 75N92021D00002, 75N92021D00003, 75N92021D00004, 75N92021D00005. Genome sequencing for  
595 “NHLBI TOPMed: Whole Genome Sequencing and Related Phenotypes in the Women’s Health  
596 Initiative Study (WHI)” (phs001237) was performed at Broad Institute of MIT and Harvard Genomics

597 Platform (HHSN268201500014C). Support for the Diabetes Heart Study (DHS) by R01 HL92301, R01  
598 HL67348, R01 NS058700, R01 AR48797, R01 DK071891, R01 AG058921, the General Clinical  
599 Research Center of the Wake Forest University School of Medicine (M01 RR07122, F32 HL085989),  
600 the American Diabetes Association, and a pilot grant from the Claude Pepper Older Americans  
601 Independence Center of Wake Forest University Health Sciences (P60 AG10484). Genome sequencing  
602 for "NHLBI TOPMed: The Diabetes Heart Study" (phs001412) was performed at the Broad Institute of  
603 MIT and Harvard Genomic Platform (HHSN268201500014C). The Atherosclerosis Risk in Communities  
604 study has been funded in whole or in part with Federal funds from the National Heart, Lung, and Blood  
605 Institute, National Institutes of Health, Department of Health and Human Services, under Contract nos.  
606 (75N92022D00001, 75N92022D00002, 75N92022D00003, 75N92022D00004, 75N92022D00005).  
607 The authors thank the staff and participants of the ARIC study for their important contributions. Whole  
608 genome sequencing (WGS) for the Trans-Omics in Precision Medicine (TOPMed) program was  
609 supported by the National Heart, Lung and Blood Institute (NHLBI). WGS for "NHLBI TOPMed:  
610 Atherosclerosis Risk in Communities (ARIC)" (phs001211) was performed at the Baylor College of  
611 Medicine Human Genome Sequencing Center (HHSN268201500015C and 3U54HG003273-12S2)  
612 and the Broad Institute for MIT and Harvard (3R01HL092577-06S1). Centralized read mapping and  
613 genotype calling, along with variant quality metrics and filtering were provided by the TOPMed  
614 Informatics Research Center (3R01HL-117626-02S1). Phenotype harmonization, data management,  
615 sample-identity QC, and general study coordination, were provided by the TOPMed Data Coordinating  
616 Center (3R01HL-120393-02S1). We gratefully acknowledge the studies and participants who provided  
617 biological samples and data for TOPMed. The Genome Sequencing Program (GSP) was funded by the  
618 National Human Genome Research Institute (NHGRI), the National Heart, Lung, and Blood Institute  
619 (NHLBI), and the National Eye Institute (NEI). The GSP Coordinating Center (U24 HG008956)  
620 contributed to cross program scientific initiatives and provided logistical and general study coordination.  
621 The Centers for Common Disease Genomics (CCDG) program was supported by NHGRI and NHLBI,  
622 and whole genome sequencing was performed at the Baylor College of Medicine Human Genome  
623 Sequencing Center (UM1 HG008898). The COPDGene study (NCT00608764) is supported by grants  
624 from the NHLBI (U01HL089897 and U01HL089856), by NIH contract 75N92023D00011, and by the  
625 COPD Foundation through contributions made to an Industry Advisory Committee that has included  
626 AstraZeneca, Bayer Pharmaceuticals, Boehringer-Ingelheim, Genentech, GlaxoSmithKline, Novartis,  
627 Pfizer and Sunovion. A full listing of COPDGene investigators can be found at:  
628 <http://www.copdgene.org/directory>. Genome sequencing for "NHLBI TOPMed: Genetic Epidemiology  
629 of COPD Study" (phs000951) was performed at Northwest Genomics Center and Broad Genomics  
630 (3R01HL089856-08S1, HHSN268201500014C, HHSN268201500014C). This Cardiovascular Health  
631 Study research was supported by NHLBI contracts HHSN268201200036C, HHSN268200800007C,  
632 HHSN268201800001C, N01HC55222, N01HC85079, N01HC85080, N01HC85081, N01HC85082,  
633 N01HC85083, N01HC85086, 75N92021D00006; and NHLBI grants U01HL080295, R01HL087652,  
634 R01HL105756, R01HL103612, R01HL120393, and U01HL130114 with additional contribution from the  
635 National Institute of Neurological Disorders and Stroke (NINDS). Additional support was provided  
636 through R01AG023629 from the National Institute on Aging (NIA). Genome sequencing for "NHLBI  
637 TOPMed: Cardiovascular Health Study" (phs001368.v2.p1) was performed at the Baylor College of  
638 Medicine Human Genome Sequencing Center (3U54HG003273-12S2, HHSN268201500015C,  
639 HHSN268201600033I). A full list of principal CHS investigators and institutions can be found at CHS-  
640 NHLBI.org. The TOPMed component of the Amish Research Program was supported by NIH grants  
641 R01 HL121007, U01 HL072515, and R01 AG18728. Genome sequencing for NHLBI TOPMed: Amish  
642 (phs000956) was performed at the Broad Institute of MIT and Harvard (3R01HL121007-01S1). The  
643 Framingham Heart Study (FHS) acknowledges the support of contracts NO1-HC-25195,  
644 HHSN268201500001I and 75N92019D00031 from the National Heart, Lung and Blood Institute and  
645 grant supplement R01 HL092577-06S1 for this research. Genome sequencing for "NHLBI TOPMed:  
646 Whole Genome Sequencing and Related Phenotypes in the Framingham Heart Study (FHS)"  
647 (phs000974) was performed at Broad Institute of MIT and Harvard Genomics Platform

648 (3U54HG003067-12S2). We also acknowledge the dedication of the FHS study participants without  
649 whom this research would not be possible. Dr. Vasan is supported in part by the Evans Medical  
650 Foundation and the Jay and Louis Coffman Endowment from the Department of Medicine, Boston  
651 University School of Medicine. GeneSTAR was supported by the National Institutes of Health/National  
652 Heart, Lung, and Blood Institute (U01 HL72518, HL087698, HL112064, HL49762, HL59684, HL58625,  
653 HL071025), by the National Institutes of Health/ National Institute of Nursing Research (NR0224103,  
654 NR008153), and by a grant from the National Institutes of Health/National Center for Research  
655 Resources (M01-RR000052) to the Johns Hopkins General Clinical Research Center. Genome  
656 sequencing for NHLBI TOPMed: GeneSTAR (Genetic Study of Atherosclerosis Risk)(phs001218) was  
657 performed at the Broad Institute of MIT and Harvard (HHSN268201500014C), at PsomaGen (formerly  
658 MacroGen, HHSN268201500014C), and at Illumina (HL112064). We gratefully acknowledge the studies  
659 and participants who provided biological samples and data for UK Biobank.

660

#### 661 **Disclosures**

662

663 Dr. Reeskamp is cofounder of Lipid Tools and reports speaker fees from Ultragenyx, Novartis, and  
664 Daiichi Sankyo. Dr. Ellinor receives sponsored research support from Bayer AG, Bristol Myers Squibb,  
665 Pfizer and Novo Nordisk; he has also served on advisory boards or consulted for Bayer AG, all unrelated  
666 to the present work. Dr. Natarajan reports research grants from Allelica, Amgen, Apple, Boston  
667 Scientific, Genentech / Roche, and Novartis, personal fees from Allelica, Apple, AstraZeneca,  
668 Blackstone Life Sciences, Creative Education Concepts, CRISPR Therapeutics, Eli Lilly & Co, Esperion  
669 Therapeutics, Foresite Labs, Genentech / Roche, GV, HeartFlow, Magnet Biomedicine, Merck, Novartis,  
670 TenSixteen Bio, and Tourmaline Bio, equity in Bolt, Candela, Mercury, MyOme, Parameter Health,  
671 Preciseli, and TenSixteen Bio, and spousal employment at Vertex Pharmaceuticals, all unrelated to the  
672 present work. Dr. Fahed reports being co-founder of Goodpath, serving as scientific advisor to MyOme  
673 and HeartFlow, and receiving a research grant from Foresite Labs, all unrelated to the present work.  
674 LMR and SSR are consultants for the NHLBI TOPMed Administrative Coordinating Center (through  
675 Westat). MHC has received grant support from Bayer and consulting fees from Apogee and BMS. The  
676 remaining authors declare no competing interests.

677

678

679

680

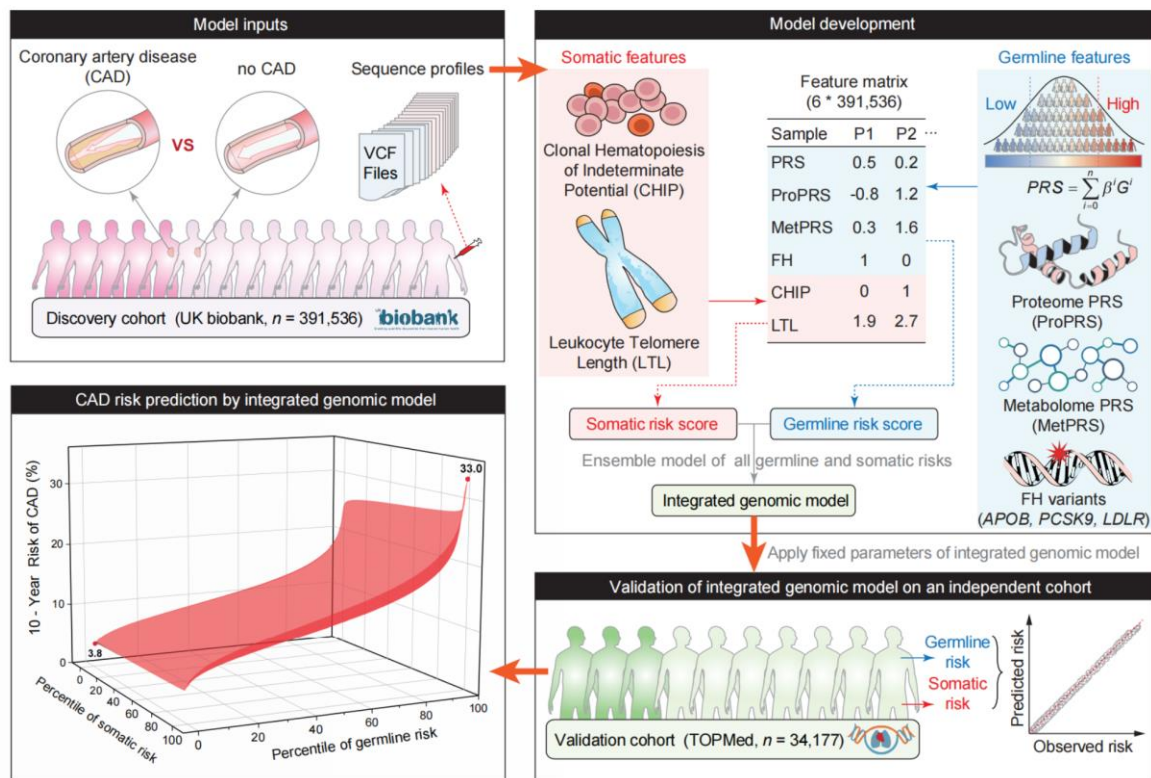
681 **References:**

- 682 1. Martin, S. S. *et al.* 2024 Heart Disease and Stroke Statistics: A Report of US and Global Data  
683 From the American Heart Association. *Circulation* **149**, (2024).
- 684 2. Fahed, A. C. & Natarajan, P. Clinical applications of polygenic risk score for coronary artery  
685 disease through the life course. *Atherosclerosis* **386**, 117356 (2023).
- 686 3. Mars, N. *et al.* Polygenic and clinical risk scores and their impact on age at onset and prediction of  
687 cardiometabolic diseases and common cancers. *Nat. Med.* **26**, 549–557 (2020).
- 688 4. Fahed, A. C. *et al.* Polygenic background modifies penetrance of monogenic variants for tier 1  
689 genomic conditions. *Nat. Commun.* **11**, 3635 (2020).
- 690 5. Khera, A. V. *et al.* Genome-wide polygenic scores for common diseases identify individuals with  
691 risk equivalent to monogenic mutations. *Nat. Genet.* **50**, 1219–1224 (2018).
- 692 6. Nakao, T. *et al.* Mendelian randomization supports bidirectional causality between telomere length  
693 and clonal hematopoiesis of indeterminate potential. *Sci. Adv.* **8**, eabl6579 (2022).
- 694 7. Haycock, P. C. *et al.* Leucocyte telomere length and risk of cardiovascular disease: systematic  
695 review and meta-analysis. *BMJ* **349**, g4227 (2014).
- 696 8. Zhao, K. *et al.* Somatic and Germline Variants and Coronary Heart Disease in a Chinese  
697 Population. *JAMA Cardiol.* **9**, 233–242 (2024).
- 698 9. Muntner, P. *et al.* Validation of the atherosclerotic cardiovascular disease Pooled Cohort risk  
699 equations. *JAMA* **311**, 1406–1415 (2014).
- 700 10. Xu, Y. *et al.* An atlas of genetic scores to predict multi-omic traits. *Nature* **616**, 123–131  
701 (2023).
- 702 11. Goff, D. C. *et al.* 2013 ACC/AHA Guideline on the Assessment of Cardiovascular Risk: A  
703 Report of the American College of Cardiology/American Heart Association Task Force on Practice  
704 Guidelines. *Circulation* **129**, (2014).
- 705 12. Patel, A. P. *et al.* A multi-ancestry polygenic risk score improves risk prediction for coronary  
706 artery disease. *Nat. Med.* **29**, 1793–1803 (2023).
- 707 13. Marston, N. A. *et al.* Predictive Utility of a Coronary Artery Disease Polygenic Risk Score in  
708 Primary Prevention. *JAMA Cardiol.* **8**, 130–137 (2023).
- 709 14. Urbut, S. M. *et al.* Dynamic Importance of Genomic and Clinical Risk for Coronary Artery  
710 Disease Over the Life Course. *MedRxiv Prepr. Serv. Health Sci.* 2023.11.03.23298055 (2023)  
711 doi:10.1101/2023.11.03.23298055.
- 712 15. Arnett, D. K. *et al.* 2019 ACC/AHA Guideline on the Primary Prevention of Cardiovascular  
713 Disease: Executive Summary. *J. Am. Coll. Cardiol.* **74**, 1376–1414 (2019).
- 714 16. Helgason, H. *et al.* Evaluation of Large-Scale Proteomics for Prediction of Cardiovascular  
715 Events. *JAMA* **330**, 725–735 (2023).
- 716 17. Carrasco-Zanini, J. *et al.* Proteomic signatures improve risk prediction for common and rare  
717 diseases. *Nat. Med.* (2024) doi:10.1038/s41591-024-03142-z.
- 718 18. Mosley, J. D. *et al.* Predictive Accuracy of a Polygenic Risk Score Compared With a Clinical  
719 Risk Score for Incident Coronary Heart Disease. *JAMA* **323**, 627–635 (2020).
- 720 19. Elliott, J. *et al.* Predictive Accuracy of a Polygenic Risk Score-Enhanced Prediction Model vs  
721 a Clinical Risk Score for Coronary Artery Disease. *JAMA* **323**, 636–645 (2020).
- 722 20. Manichaikul, A. *et al.* Robust relationship inference in genome-wide association studies.



- 723 *Bioinforma. Oxf. Engl.* **26**, 2867–2873 (2010).
- 724 21. Khera, A. V. *et al.* Diagnostic Yield and Clinical Utility of Sequencing Familial  
725 Hypercholesterolemia Genes in Patients With Severe Hypercholesterolemia. *J. Am. Coll. Cardiol.*  
726 **67**, 2578–2589 (2016).
- 727 22. Khera, A. V. *et al.* Whole-Genome Sequencing to Characterize Monogenic and Polygenic  
728 Contributions in Patients Hospitalized With Early-Onset Myocardial Infarction. *Circulation* **139**,  
729 1593–1602 (2019).
- 730 23. Reeskamp, L. F. *et al.* Polygenic Background Modifies Risk of Coronary Artery Disease  
731 Among Individuals With Heterozygous Familial Hypercholesterolemia. *JACC Adv.* **2**, 100662  
732 (2023).
- 733 24. McLaren, W. *et al.* The Ensembl Variant Effect Predictor. *Genome Biol.* **17**, 122 (2016).
- 734 25. Karczewski, K. J. *et al.* The mutational constraint spectrum quantified from variation in  
735 141,456 humans. *Nature* **581**, 434–443 (2020).
- 736 26. Barton, A. R., Sherman, M. A., Mukamel, R. E. & Loh, P.-R. Whole-exome imputation within  
737 UK Biobank powers rare coding variant association and fine-mapping analyses. *Nat. Genet.* **53**,  
738 1260–1269 (2021).
- 739 27. Yu, Z. *et al.* Genetic modification of inflammation- and clonal hematopoiesis-associated  
740 cardiovascular risk. *J. Clin. Invest.* **133**, e168597 (2023).
- 741 28. Bick, A. G. *et al.* Inherited causes of clonal haematopoiesis in 97,691 whole genomes. *Nature*  
742 **586**, 763–768 (2020).
- 743 29. Vlasschaert, C. *et al.* A practical approach to curate clonal hematopoiesis of indeterminate  
744 potential in human genetic data sets. *Blood* **141**, 2214–2223 (2023).
- 745 30. Codd, V. *et al.* Measurement and initial characterization of leukocyte telomere length in  
746 474,074 participants in UK Biobank. *Nat. Aging* **2**, 170–179 (2022).
- 747 31. Chang, C. C. *et al.* Second-generation PLINK: rising to the challenge of larger and richer  
748 datasets. *GigaScience* **4**, 7 (2015).
- 749 32. the Million Veteran Program *et al.* Genetic analysis of over 1 million people identifies 535 new  
750 loci associated with blood pressure traits. *Nat. Genet.* **50**, 1412–1425 (2018).
- 751 33. Tobin, M. D., Sheehan, N. A., Scurrah, K. J. & Burton, P. R. Adjusting for treatment effects in  
752 studies of quantitative traits: antihypertensive therapy and systolic blood pressure. *Stat. Med.* **24**,  
753 2911–2935 (2005).
- 754





755

756 **Fig. 1.** Overview of development and validation of integrated genomic model (IGM). Based on  
 757 sequencing data from UK Biobank ( $N=391,536$ ), we curated 6 genomic features that are associated  
 758 with the risk of CAD. Scores of somatic and germline risks were ensemble to construct IGM, which  
 759 was then validated in the TOPMed cohort ( $N=34,177$ ).

760

761

762

763

764

765

766

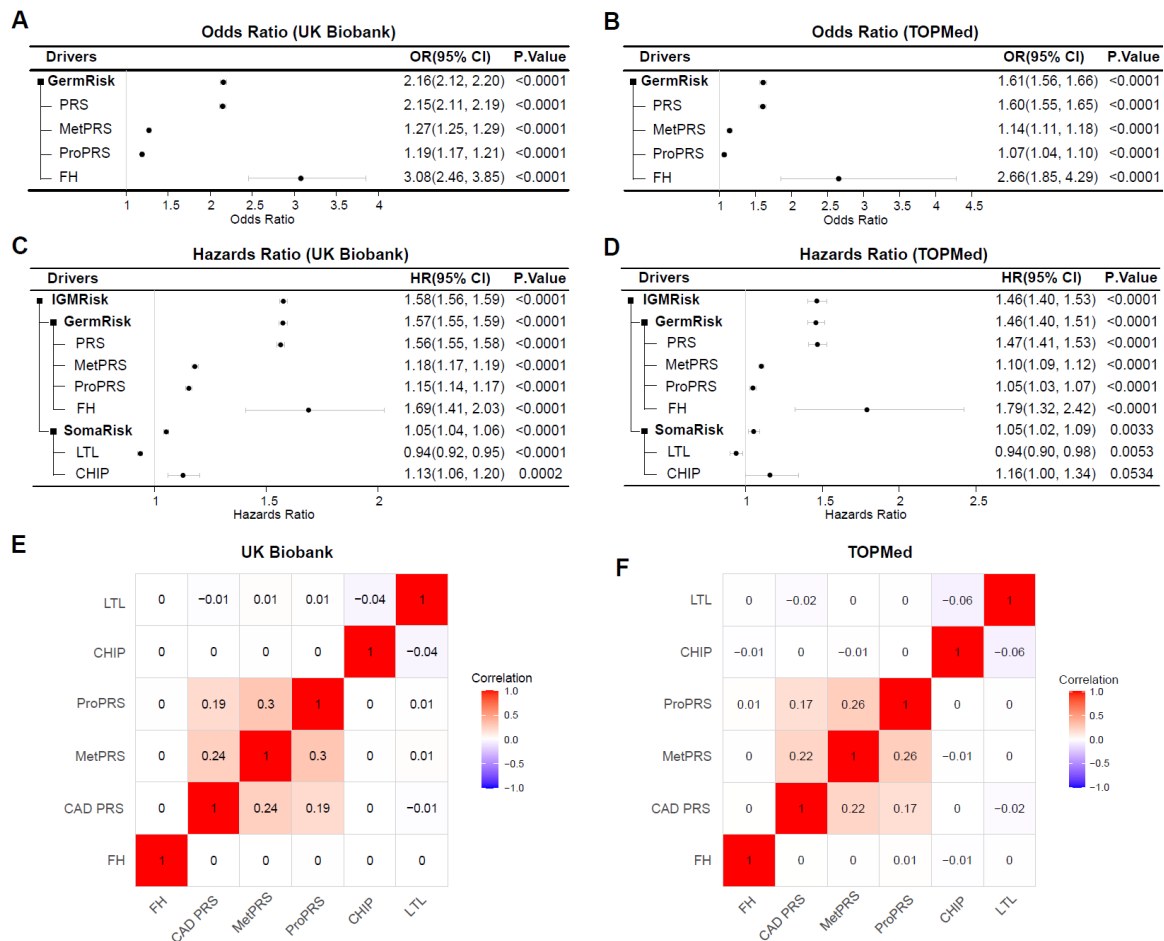
767

768

769

770

771



772

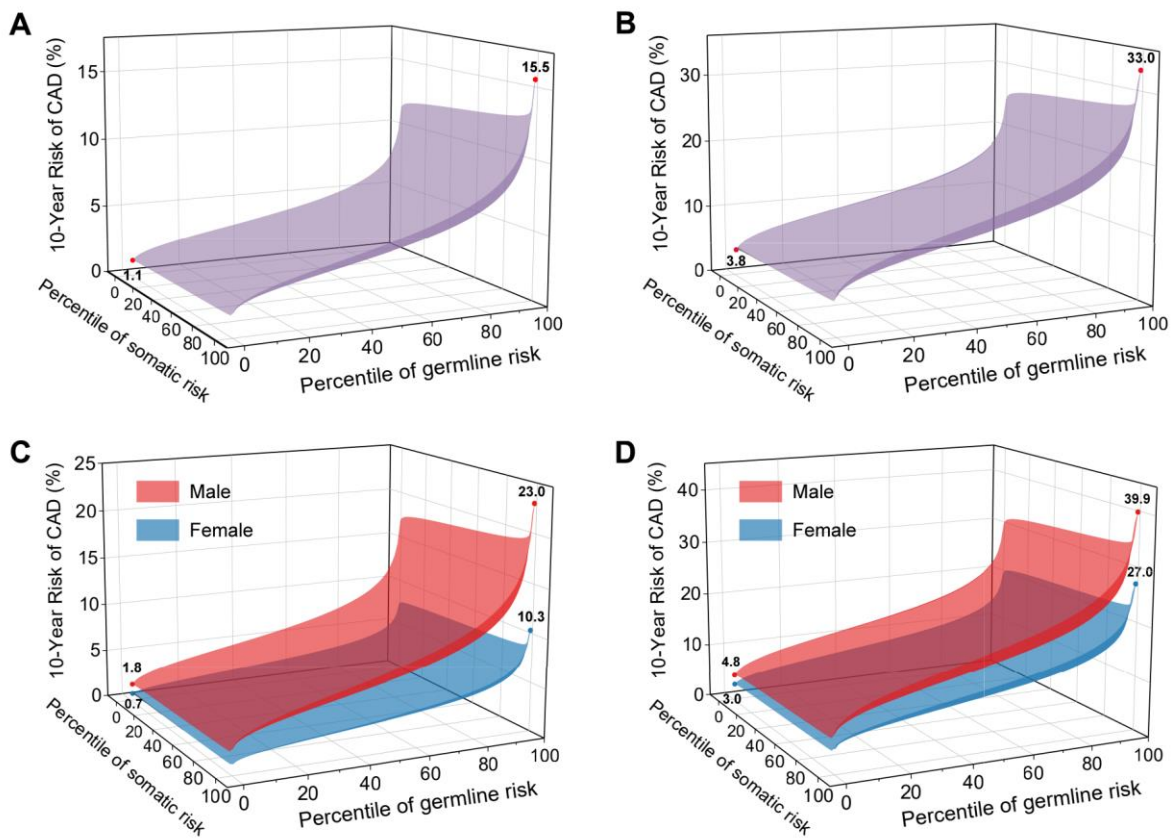
773 **Fig. 2.** Effect size of genomic drivers in UK Biobank and TOPMed. Effect sizes based on prevalent  
 774 coronary artery disease (CAD) in UK Biobank (A) and TOPMed (B), and incident CAD in UK Biobank  
 775 (C) and TOPMed (D) are presented. Odds ratio and hazard ratio per standard deviation are shown for  
 776 all continuous measures (PRS, MetPRS, ProPRS, LTL, GermRisk, SomaRisk, IGMRisk). Odds ratio  
 777 and hazard ratio per carrier status are shown for FH and CHIP. Estimates are derived from logistic  
 778 regression (panels A and B) or Cox proportional hazards model (panels C and D) with sex, recruitment  
 779 age, and the first 10 principal components of genetic ancestry as covariates. GermRisk is a weighted  
 780 combination of four genetic drivers (PRS, MetPRS, ProPRS, and FH) as a single predictor, with weights  
 781 estimated by a logistic regression model. SomaRisk is a weighted combination of two somatic drivers  
 782 (CHIP and LTL) as a single predictor, with weights estimated by a Cox proportional hazards model.  
 783 IGMRisk is a combination of GermRisk and SomaRisk, weighted from a Cox proportional hazards  
 784 regression model estimation. Correlations among the six genetic drivers are shown for the UK Biobank  
 785 (E) and TOPMed (F). CI, confidence interval; PRS, polygenic risk score (PRS) for CAD; MetPRS,  
 786 metabolome PRS; ProPRS, proteome PRS; LTL, leukocyte telomere length; FH, familial  
 787 hypercholesterolemia variants; CHIP, clonal hematopoiesis of indeterminate potential.

788

789

790

791



792

793 **Fig. 3.** Ten-year risk of CAD as a function of somatic and germline risk from the integrated model. Ten-  
794 year risk of CAD among all participants from UK Biobank (A) and TOPMed (B), and sex-stratified 10-  
795 year risks of CAD in UK Biobank (C) and TOPMed (D) are presented.

796

797

798

799

800

801

802

803

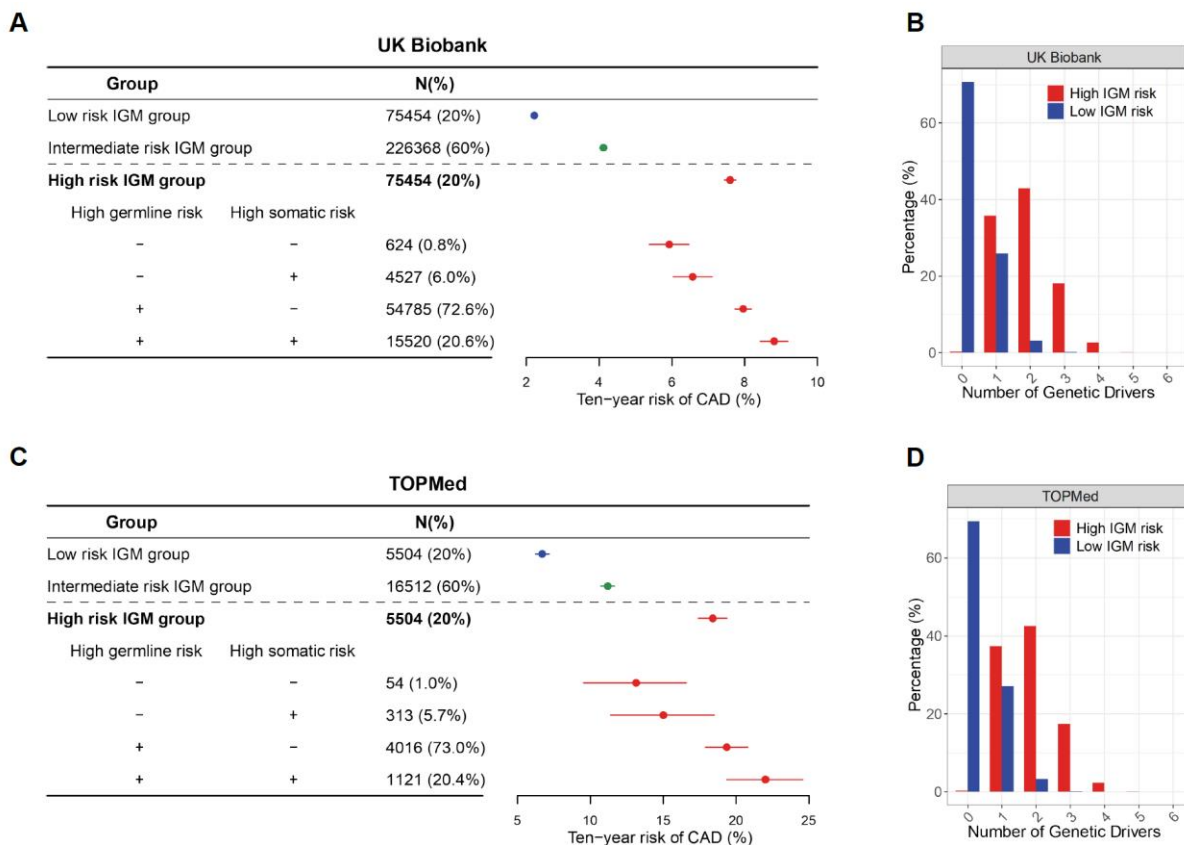
804

805

806

807

808



809

810 **Fig. 4.** The integrated genomic model (IGM) captures participants with diverse genetic risk profiles  
 811 contributing to risk in the UK Biobank (**A, B**) and TOPMed (**C, D**). (**A**) and (**C**), The ten-year risk of CAD  
 812 was estimated for each IGM risk group in the UK Biobank and TOPMed dataset. Categories were  
 813 defined as low risk (bottom 20%), intermediate risk (middle 60%), and high risk group (top 20%). In the  
 814 high risk group, the genetic profile was further partitioned by the status of carrying a high germline risk  
 815 or high somatic risk. The high germline risk was defined as the top 20% with a composite risk estimated  
 816 from four germline genetic risk drivers (FH, PRS, MetPRS, and ProPRS). The high somatic risk was  
 817 defined as the top 20% with a composite risk estimated from two somatic risk drivers (CHIP and LTL).  
 818 (**B**) and (**D**), the genetic risk profiles for the IGM low risk (bottom 20%) and high risk (top 20%) groups,  
 819 respectively. The six drivers are FH, PRS, MetPRS, ProPRS, CHIP, and LTL. The continuous variables  
 820 were binarized, with individuals in the top 20% treated as carriers, except for LTL (the bottom 20% were  
 821 treated as carriers). PRS, polygenic risk score (PRS) for CAD; MetPRS, metabolome PRS; ProPRS,  
 822 proteome PRS; LTL, leukocyte telomere length; FH, familial hypercholesterolemia variants; CHIP,  
 823 clonal hematopoiesis of indeterminate potential.

824

825

826

827

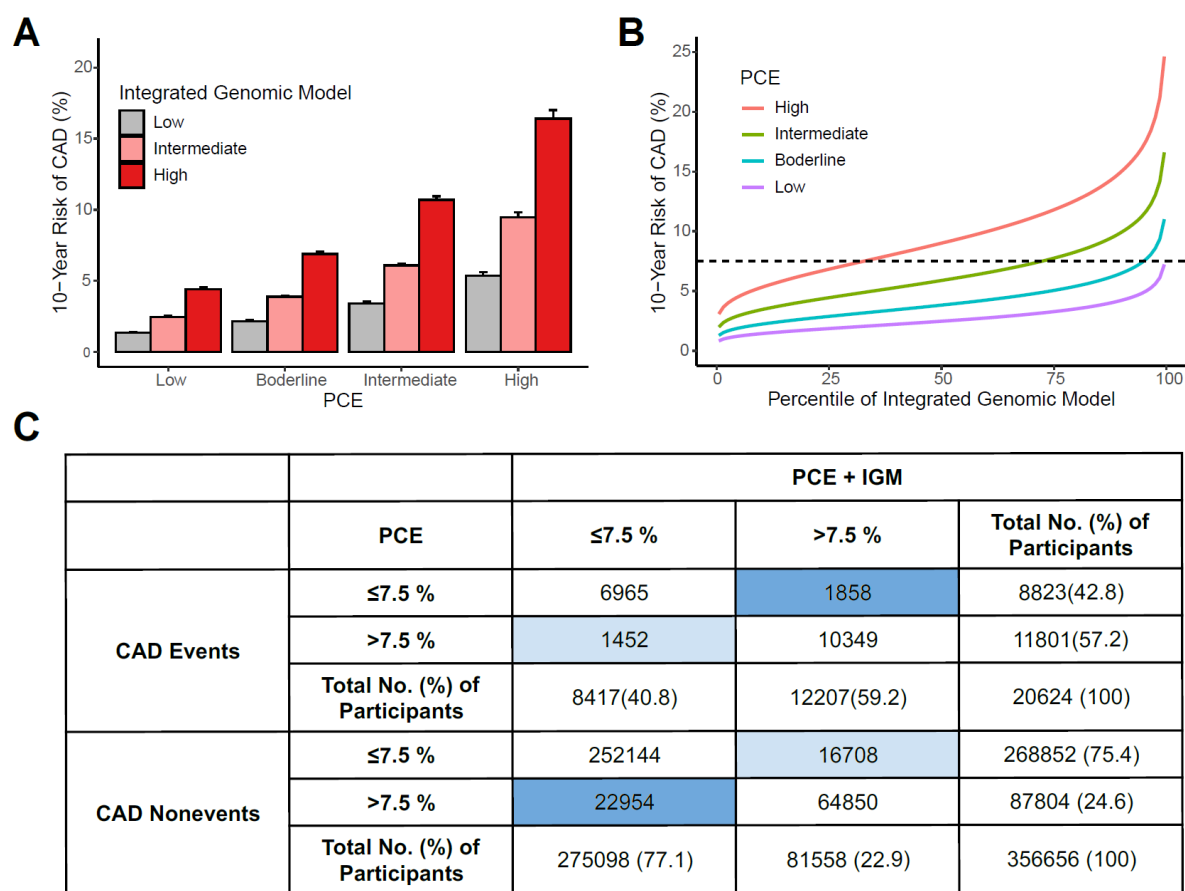
828

829

830

831

832



833

834 **Fig. 5.** Stratification (**A, B**) and reclassification (**C**) of 10-year predicted CAD risk based on IGM. **A,**  
 835 stratification by IGM risk within PCE risk stratum. **B,** Predicted 10-year CAD risk gradient by genetic  
 836 risk percentile. **C,** Reclassification of 10-year predicted CAD risk—columns and rows indicate categories  
 837 of 10-year predicted risk, with the number of individuals in each risk category, the number of samples  
 838 correctly reclassified and wrongly reclassified are in dark and light blue, respectively. A continuous net  
 839 reclassification index was 33.45% (95% CI, 32.11%-34.76%). IGM categories were defined as low risk  
 840 (bottom 20%), intermediate risk (middle 60%), and high risk group (top 20%), respectively. PCE  
 841 categories were defined as low (estimated risk less than 5%), borderline (risk between 5% to 7.5%),  
 842 intermediate (risk between 7.5% and 20%), and high (risk greater than 20%), respectively. IGM:  
 843 integrated genomic model; PCE, pooled cohort equation.

844

845

846

847

848

849

850

851

852

853